



LIQUEFACTION CHARACTERISTIC OF UNDISTURBED VOLCANIC SOIL IN CYCLIC TRIAXIAL TEST

Motoyuki SUZUKI¹, Tetsuro YAMAMOTO²

SUMMARY

Shirasu is a Japanese volcanic soil and mainly distributed in the southern Kyushu. The Shirasu has a crushability of brittle soil particle. In the Shirasu deposit ground, liquefaction occurred during the 1997 northwestern Kagoshimaken earthquake. Reliquefaction also occurred during the aftershock. This paper describes liquefaction and reliquefaction characteristics of the Shirasu, based on results of cyclic triaxial tests on undisturbed and disturbed samples. Especially changes in void ratio and strength of the undisturbed specimens after the first liquefaction were discussed in terms of initial effective confining stress and relative density.

INTRODUCTION

Shirasu is a Japanese volcanic soil and is mainly distributed in the southern Kyushu. The thick and broad plateaus in Kagoshima prefecture are formed by the Shirasu deposits. The Shirasu has an essential feature of a porous solid resulting from a pyroclastic material. The Shirasu generally gives a lower value of density of soil particles as compared with that of other sandy soils. It is noteworthy that the Shirasu has crushability due to the brittleness of the soil particles. The Shirasu have been recently used as a reclamation material. Therefore liquefaction characteristics of the Shirasu and liquefaction potential of the Shirasu deposit ground have been examined by many researchers (e.g. Umehara et al [1]). In fact, sand boil in a dry river bed and settlement of bridge pier occurred during the 1968 Ebino earthquake (Yamanouchi [2]) and liquefaction of ground reclaimed by Shirasu occurred during the 1997 northwestern Kagoshimaken earthquake (Okabayashi et al [3]). Especially it was reported that reliquefaction occurred in a Shirasu ground which had once liquefied during the main shock (Yamamoto et al [4]). The liquefaction characteristics of disturbed sample of the Shirasu have examined in terms of the crushability of the soil particles (Hyodo et al [5]). It is important to clarify the liquefaction characteristics of undisturbed sample of the Shirasu in order to propose valid countermeasures for liquefaction in the Shirasu ground.

¹ Research Associate, Yamaguchi University, Ube, Yamaguchi, Japan, msuzuki@yamaguchi-u.ac.jp

² Professor, Yamaguchi University, Ube, Yamaguchi, Japan, tyamamot@yamaguchi-u.ac.jp

The liquefaction characteristics of Shirasu have been clarified as follows. O-hara et al [6] reported that the liquefaction strength of undisturbed sample is higher than that of disturbed sample. Okabayashi et al [7] reported that the cyclic shear behavior is significantly different from that of Toyoura sand, the influence of effective confining pressure on the cyclic shear behavior is dependent on the initial relative density and the cyclic shear strength of loose sample increases with increasing the effective confining pressure contrary to that of dense specimen. Nakata et al [8] mentioned that mechanical behavior of crushable soils such as Shirasu, Masado etc could be expressed by changes in strength due to density increase of specimen and crushability of soil particles. Finn et al [9] reported that liquefaction strength of saturated sand becomes lesser than first liquefaction strength of same sand based on the results of the shaking table and triaxial compression tests. Furthermore this finding is supported by field survey by Yasuda and Tohno [10]. O-hara and Yamamoto [11] however pointed out that the decrease in liquefaction strength result from necking of specimen experimentally generated near a top cap during first liquefaction. Therefore the liquefaction characteristics of the Shirasu have been hardly clarified.

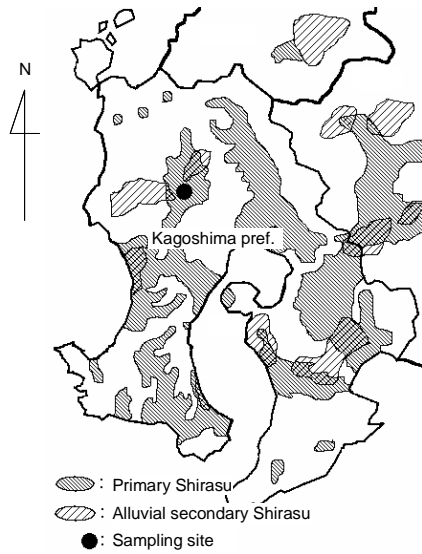


Figure 1 Distribution of Shirasu in south region of Kyushu¹²⁾

Table 1 Physical properties of Shirasu

ρ_s (g/cm ³)	U_c	D_{50} (mm)	D_{max} (mm)	e_{max}	e_{min}	F_c (%)	F_{clay} (%)
2.448	-	0.134	4.750	1.902	0.981	37.4	16.2

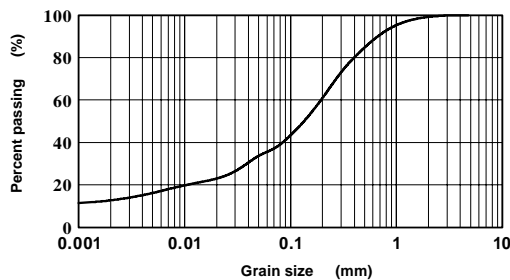


Figure 2 Grading curve of Shirasu



Photographs 1 Sampling undisturbed Shirasu

This paper describes liquefaction and reliquefaction characteristics of the Shirasu based on results of cyclic triaxial tests on undisturbed and disturbed samples. The discussion will focus on both changes in void ratio and liquefaction strength of undisturbed specimens after the first liquefaction as related to influences of the initial effective confining stress and the initial relative density.

SOIL SAMPLES AND TEST PROCEDURE

Figure 1 show distribution of Shirasu in the south area of Kyushu [12]. The undisturbed Shirasu used in this study was sampled in Hirakawa, Miyanojyo-cho, Kagoshima pref. The Shirasu used is classified into a primary Shirasu which have never been eroded and conveyed in long geological history. The progress sampling soil blocks was shown in Photographs 1 (a) to (c). Disturbed samples were sampling at the same site. In laboratory the disturbed samples were passed through the sieve 475 μm and then removed the containing tree roots. Table 1 shows physical properties of the disturbed samples used. Figure 2 shows grading curve of the disturbed samples. Physical property of disturbed sample is identified with that of undisturbed samples. The density of soil particles of the disturbed sample is 2.448 g/cm^3 . The density of soil particles of Shirasu generally varied from 2.3 to 2.5 g/cm^3 . Maximum and minimum void ratios, e_{max} and e_{min} , were respectively determined from the disturbed samples. Average value of initial void ratio, e_0 is 1.138 and a deviation of the initial void ratio, Δe_0 is 0.149. Strength parameter in termes of effective stress, $\phi' = 39.9^\circ$ and $c' = 0$ kPa are obtained from consolidated undrained triaxial compression test on the disturbed samples.

Cyclic triaxial tests were performed on both the undisturbed and the disturbed samples. Air-dried sample was filled in a cone shaped slender funnel having a nozzle. The sample was spreading in a split mould until the mould becomes filled with the sample. Tapping energy was applied by hitting the side of the mould to obtain a required density. The undisturbed specimen was cut form a frozen soil block using a core cutter circulating a refrigerant. The dimension of the specimen is 10.5 cm in height and 5 cm in diameter. After the sample is encased in the membrane with the top cap, CO_2 gas was poured into the specimen during 20 minutes for disturbed sample or 120 minutes for undisturbed sample. Subsequently

Table 2 Test cases and results on disturbed samples

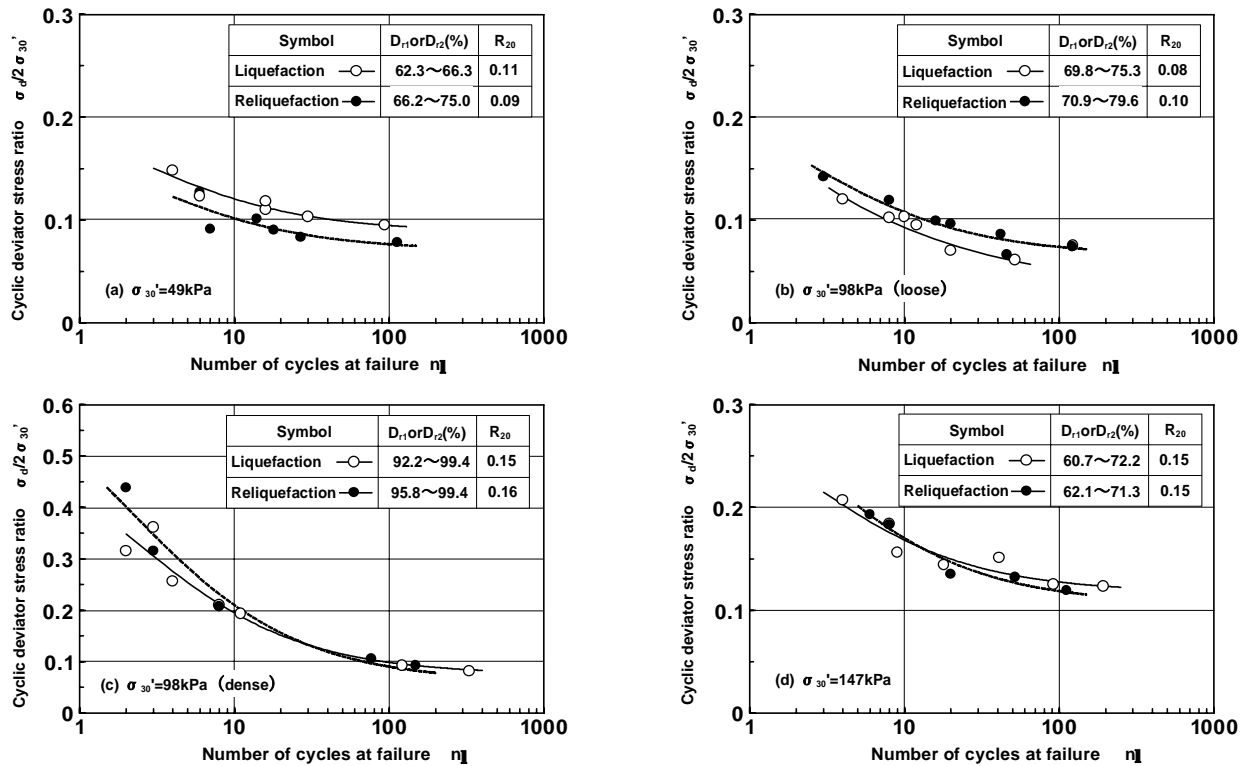
Test No.	Initial condition			At liquefaction				At reliquefaction			
	$D_{r0}(\%)$	$\sigma_{30}(\text{kPa})$	B value	$D_{r1}(\%)$	$\sigma_d/2\sigma_{30}$	$\Delta u/\sigma_{30}$	n_f	$D_{r2}(\%)$	$\sigma_d/2\sigma_{30}$	$\Delta u/\sigma_{30}$	n_f
D-1	57.5	49	0.99	62.3	0.095	1.00	94	72.1	0.078	1.00	113
D-2	62.0	49	0.95	66.3	0.103	0.99	30	75.0	0.083	0.98	27
D-3	59.1	49	0.99	62.7	0.110	1.00	16	70.8	0.090	0.99	18
D-4	62.8	49	0.98	66.2	0.118	1.00	16	74.9	0.101	0.98	14
D-5	57.2	49	0.97	62.6	0.123	0.98	6	69.5	0.091	0.97	7
D-6	58.8	49	0.97	63.1	0.148	0.97	4	66.2	0.127	0.96	6
D-7	67.7	98	0.99	74.5	0.075	0.98	123	79.6	0.086	0.97	42
D-8	63.1	98	1.00	71.3	0.061	1.00	52	75.0	0.066	0.99	46
D-9	65.9	98	1.00	73.7	0.070	0.97	20	77.0	0.074	0.98	122
D-10	65.5	98	1.00	75.3	0.095	1.00	12	76.8	0.096	0.99	20
D-11	64.2	98	1.00	71.8	0.103	1.00	10	74.4	0.099	1.00	16
D-12	64.5	98	0.98	72.1	0.102	1.00	8	74.6	0.119	0.98	8
D-13	62.2	98	1.00	69.8	0.120	0.97	4	70.9	0.142	0.96	3
D-14	58.3	147	0.96	68.2	0.123	0.99	193	69.3	0.119	0.99	112
D-15	62.0	147	0.95	72.2	0.125	0.98	92	-	-	-	-
D-16	55.8	147	0.97	60.7	0.151	0.99	41	62.1	0.135	0.99	20
D-17	63.0	147	0.97	70.0	0.144	0.97	18	70.7	0.132	0.96	52
D-18	59.5	147	0.95	69.5	0.156	0.99	9	-	-	-	-
D-19	60.4	147	0.95	70.7	0.184	0.98	8	71.3	0.183	0.99	8
D-20	58.4	147	0.95	69.0	0.207	0.97	4	70.2	0.193	0.98	6
D-21	88.7	98	0.95	92.2	0.081	0.99	331	96.2	0.092	0.99	149
D-22	88.3	98	0.99	92.5	0.092	0.98	122	95.8	0.105	0.97	77
D-23	92.8	98	0.95	97.4	0.193	0.93	11	-	-	-	-
D-24	90.4	98	0.95	94.7	0.210	0.96	8	95.8	0.207	0.97	8
D-25	92.0	98	0.96	96.2	0.256	0.96	4	97.8	0.315	0.96	3
D-26	91.3	98	0.94	97.8	0.361	0.97	3	99.4	0.438	0.91	2
D-27	91.4	98	0.98	99.4	0.315	0.96	2	-	-	-	-

de-aired water was poured into the specimen. Full saturation was checked by ensuring attainment of a B value greater than 0.95 by means of back pressure application. In the triaxial cell, the specimen was normally consolidated under a required isotropic stress and then be applied by cyclic deviator stress, σ_d having frequency of 0.1 Hz until double-amplitude axial strain, DA attain 5 %. If we carried out reliquefaction test, then the specimen was reconsolidated for 30 minutes to dissipate excess pore water pressure generated during first liquefaction.

LIQUEFACTION AND RELIQUEFACTION CHARACTERISTICS OF SHIRASU

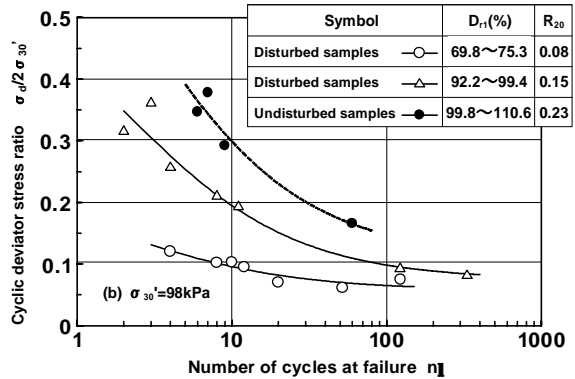
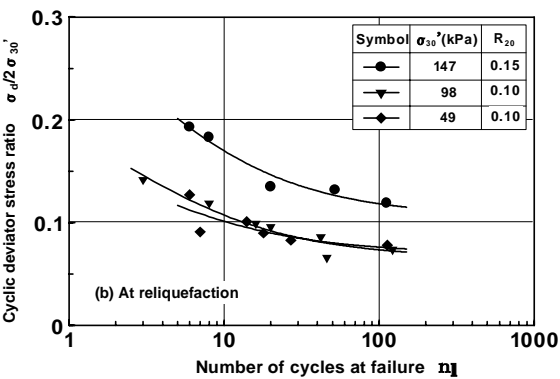
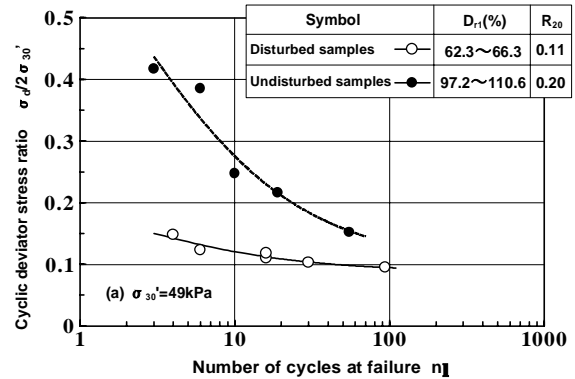
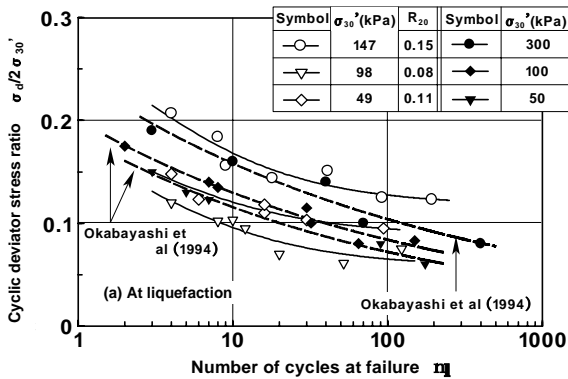
Behavior of disturbed sample

Table 2 shows test cases and results of the disturbed samples prepared with different initial relative density, D_{r0} and initial effective confining stress, σ_{30}' . Figures 3 (a) to (d) show the liquefaction and reliquefaction strength curves obtained from the test results on the disturbed samples. Table in each figure shows the relative density of specimen before liquefaction and reliquefaction, D_{r1} and D_{r2} , and cyclic deviator stress ratio, R_{20} when the specimen liquefied at number of cycles, $n_1=20$. As can be seen in Figs.3 (a), in the case of $\sigma_{30}'=49$ kPa the reliquefaction strength becomes lower value as compared with that of the first liquefaction strength. The data plotted in Figs.3 (b) and (c) are obtained from the specimen prepared with different D_{r0} under $\sigma_{30}'=98$ kPa. The reliquefaction strength of the loose specimen becomes higher than the first liquefaction strength. The reliquefaction strength of the dense specimen becomes almost equivalent to the first liquefaction strength. As shown in Figs.3 (d), there exists no clear difference between the first liquefaction and the reliquefaction strength curves under $\sigma_{30}'=147$ kPa. Figures 4 (a) and (b) show the first liquefaction and the reliquefaction strength curves of the disturbed sample under conditions of different σ_{30}' , respectively. The data are same as those in Figs.3. Each specimen was prepared for $D_{r0}=60\%$. Table 2 shows the initial relative density of the specimen. As can be seen in Figs.4



Figures 3 Liquefaction and reliquefaction strength curves for disturbed samples

(a), the liquefaction strength curves in $\sigma_{30}'=147$ kPa is higher than those in $\sigma_{30}'=49$ and 98 kPa. A part of data plotted in this figure is taken from Okabayashi et al [7]. The data are obtained from cyclic triaxial test on Shirasu under $D_{r0}=50\%$ and $\sigma_{30}'=50, 100, 300$ kPa. The liquefaction strength curves obtained from the loose specimens increases with increasing the initial effective confining pressure. It must be emphasized that the reliquefaction strength as well as the first liquefaction strength is affected by the initial effective confining pressure. This finding suggested that the soil particles which have never crushed may be newly crushed during reshearing. The liquefaction strength curve of the Shirasu varies within the ordinary range of the effective confining stress (e.g. Okabayashi et al [7]).



Figures 4 Dependency of σ_{30}' for disturbed samples

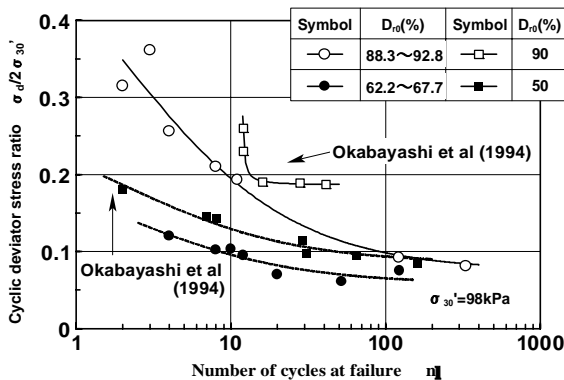
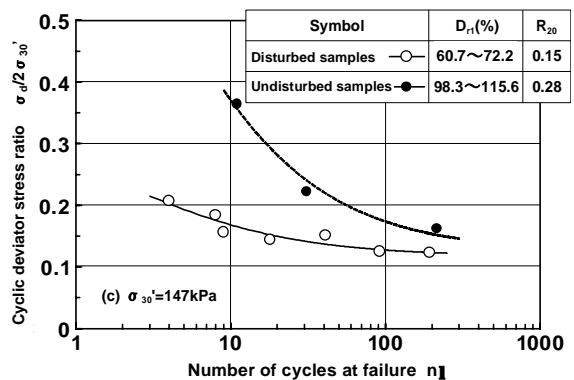


Figure 5 Dependency of D_{r0} for disturbed samples



Figures 6 Liquefaction strength curves for disturbed and undisturbed samples

Table 3 Test cases and results on undisturbed samples

Test No.	Initial condition			At liquefaction				At reliquefaction			
	D_{r0} (%)	σ_{30}' (kPa)	B value	D_{r1} (%)	$\sigma_d/2\sigma_{30}'$	$\Delta u/\sigma_{30}'$	n_f	D_{r2} (%)	$\sigma_d/2\sigma_{30}'$	$\Delta u/\sigma_{30}'$	n_f
U-1	97.2	49	0.93	99.8	0.216	0.96	19	103.8	0.228	0.94	7
U-2	108.7	49	0.87	110.6	0.247	1.00	10	114.8	0.259	1.00	7
U-3	96.2	49	0.87	97.2	0.152	1.00	55	102.2	0.201	1.00	19
U-4	103.6	49	0.90	105.0	0.417	0.99	3	109.1	0.397	0.98	3
U-5	95.8	98	0.79	98.5	0.385	0.95	6	109.9	0.381	0.95	3
U-6	108.7	98	0.74	110.6	0.378	1.00	7	114.8	0.368	0.99	5
U-7	97.2	98	0.74	99.8	0.292	0.99	9	103.8	0.312	1.00	11
U-8	103.6	98	0.80	106.0	0.347	1.00	6	108.7	0.352	0.98	4
U-9	99.1	98	0.83	101.8	0.166	1.00	60	105.8	0.188	1.00	18
U-10	108.9	147	0.85	112.1	0.222	1.00	31	116.5	0.225	1.00	11
U-11	102.4	147	0.69	105.6	0.364	1.00	11	-	-	-	-
U-12	110.6	147	0.88	115.6	0.162	1.00	215	116.6	0.171	1.00	23
U-13	94.7	147	0.90	98.3	0.192	1.00	19	102.5	0.195	1.00	15
U-14	90.9	196	0.91	94.7	0.342	0.99	6	96.2	0.343	0.97	4
U-15	92.9	196	0.90	97.0	0.295	0.98	8	97.5	0.298	0.97	9
U-16	94.5	196	0.85	98.9	0.267	0.99	17	100.2	0.274	0.85	12
U-17	94.9	196	0.89	99.1	0.229	1.00	23	101.8	0.229	1.00	18
U-18	89.6	196	0.89	94.2	0.166	1.00	86	102.8	0.164	0.98	16

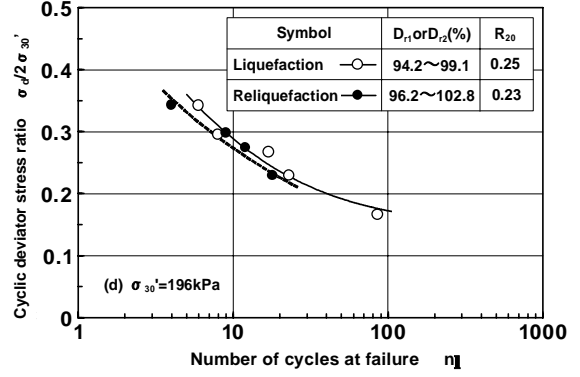
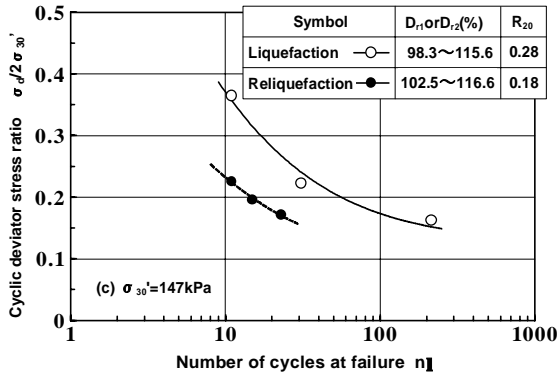
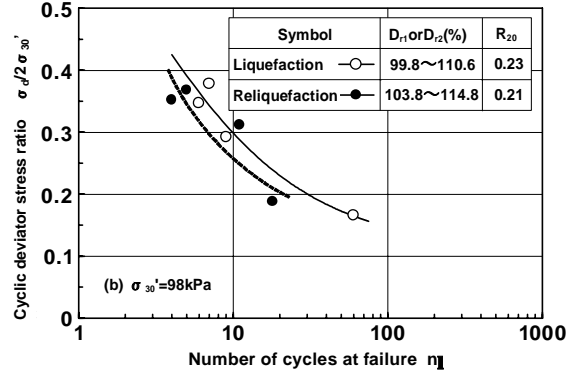
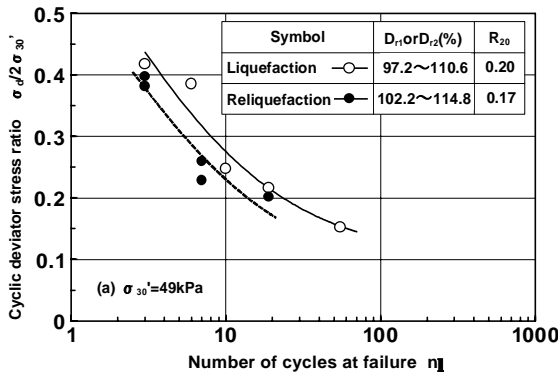
This tendency is attributable to difference in the degree of crushability in isotropic consolidation process (Nakata et al [8]). Figure 5 shows the liquefaction strength curves of the disturbed samples under condition of different D_{r0} . All tests were carried out under $\sigma_{30}'=98$ kPa. The open and the closed circles used in this figure correspond to $D_{r0}=88.3\sim 92.8\%$ ($D_{r1}=92.2\sim 99.4\%$) and $D_{r0}=62.2\sim 67.7\%$ ($D_{r1}=69.8\sim 75.3\%$), respectively. As compared with the data from Okabayashi et al [7], the shape of the liquefaction strength curve is significantly changed by the initial relative density. The liquefaction strength curve of the higher D_{r0} sample becomes higher than that of the lower D_{r0} sample.

Behavior of undisturbed sample

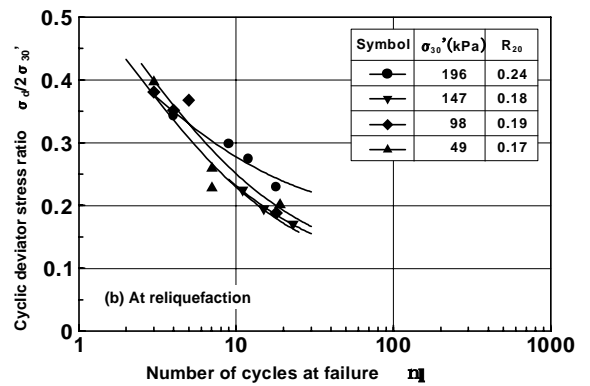
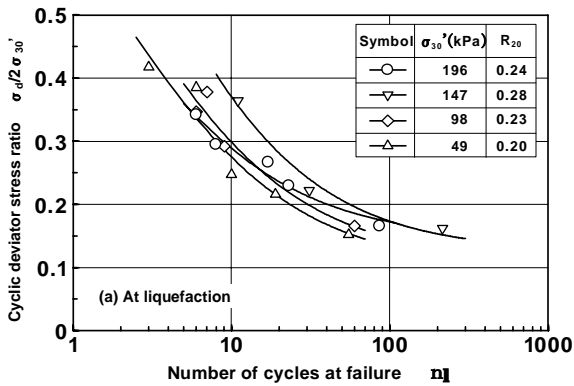
Table 3 shows the cases and results of cyclic triaxial test on undisturbed samples under different initial confining pressure. Figures 6 (a) to (c) show the liquefaction strength curves of the disturbed and the undisturbed samples in the case of $\sigma_{30}'=49, 98, 147$ kPa. Since the relative density of the undisturbed sample immediately after the isotropic consolidation is different from that of the disturbed sample, it is not reasonable to compare the liquefaction strength of the undisturbed samples with that of the disturbed samples. As can be seen in Figs.6 (b), the liquefaction strength of the undisturbed sample is generally higher than that of the disturbed samples. Figures 7 (a) to (d) show the first liquefaction and reliquefaction strength curves of the undisturbed samples in the case of $\sigma_{30}'=49, 98, 147, 196$ kPa, respectively. As can be seen in Figs.7 (a) and (b), the reliquefaction strength is lower than that of the first liquefaction strength. Especially there exists a clear difference between the first liquefaction and the reliquefaction strength in the case of $\sigma_{30}'=147$ kPa. Such a difference is not obvious in the case of $\sigma_{30}'=196$ kPa. This may be due to loss of cementation between the soil particles during the first liquefaction. Figures 8 (a) and (b) show the first liquefaction and reliquefaction strength curves of the undisturbed samples respectively. Except for $\sigma_{30}'=196$ kPa, the liquefaction strength curves moved upward accompanying the increase of the initial effective confining stress. This finding proved the dependency of effective confining stress for loose sample. On the other hand, the reliquefaction strength curves seem not to be affected by the effective confining stress.

Change in density of specimen due to reconsolidation after liquefaction

Change in void ratio after the first liquefaction is discussed based on the test results on the disturbed and the undisturbed samples. Figures 9 (a) and (b) show change rate of the void ratio, $\Delta e/e_1$ for both samples. Here e_1 and e_2 are respectively the void ratio after consolidation and liquefaction. The change in void ratio, Δe is defined as e_1-e_2 . As shown in Figs.9 (a), $\Delta e/e_1$ of the disturbed samples decreases with the decreasing



Figures 7 Liquefaction and reliquefaction strength curves for undisturbed samples



Figures 8 Dependency of σ_{30}' for undisturbed samples

σ_{30}' . The undisturbed sample has a similar tendency to the disturbed sample. The void ratio of the disturbed sample artificially varied from 1.262 to 1.356. On the other hand, the void ratio of the undisturbed samples is widely distributed in the range of 1.060 to 1.256. Therefore the undisturbed sample is situated on denser condition than the disturbed sample. The main reason is that the change in void ratio during reconsolidation seems to be affected by the initial fabric of the sample. During reconsolidation after liquefaction, the change in void ratio of the disturbed sample is bigger than that of the undisturbed sample. Energy required to liquefaction, w_1 which is defined as the product of the cyclic deviator stress ratio, $\sigma_d/(2\sigma_{30}')$ and the logarithm of n_1 on a liquefaction strength curve, is expressed by equation (1).

$$w_1 = \left(\frac{\sigma_d}{2\sigma_{30}'} \right) \cdot \log n_f \quad (1)$$

The energy required to reliquefaction, w_2 as well as w_1 is defined by the equation (1). On the other hand, the plastic energy, W_p , during cyclic shearing is expressed by equation (2).

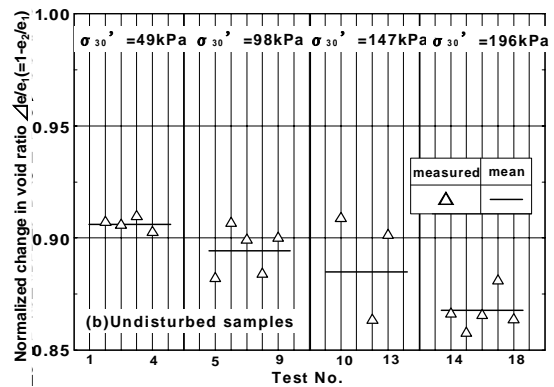
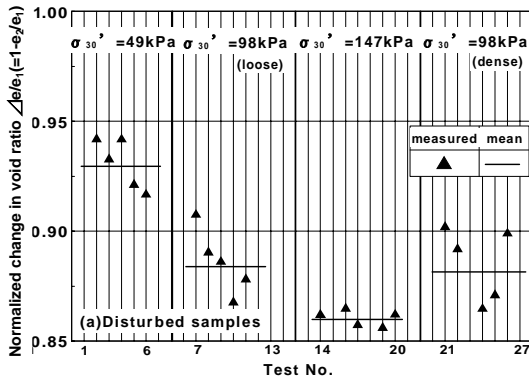
$$W_p = \int p' d\varepsilon_v + \int q d\varepsilon_s \quad (2)$$

Here p' is the mean effective principle stress, q is the principle stress difference, ε_v is the volumetric strain and ε_s is the shear strain. They are expressed by following equations (3) to (6).

$$p' = \frac{\sigma_1' + 2\sigma_3'}{3} \quad (3)$$

$$q = \sigma_1 - \sigma_3 \quad (4)$$

$$\varepsilon_v = \varepsilon_1 + 2\varepsilon_3 \quad (5)$$



Figures 9 Normalized change in void ratio for disturbed and undisturbed samples

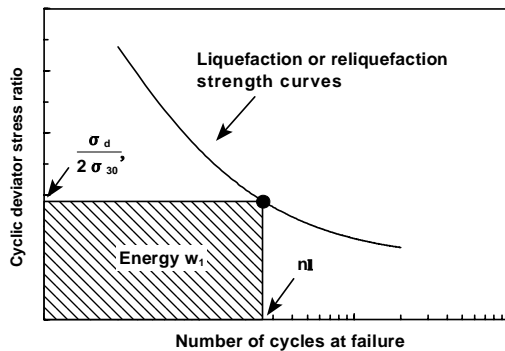


Figure 10 Definition of w_1

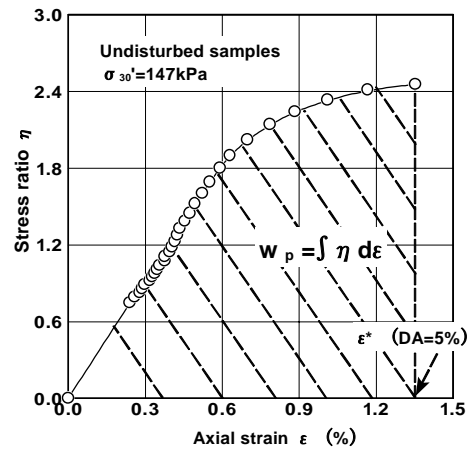


Figure 11 $\eta \sim \varepsilon$ curve to calculate w_p

$$\varepsilon_s = \frac{2}{3}(\varepsilon_1 - \varepsilon_3) \quad (6)$$

Plastic energy normalized by p' , w_p is expressed by equation (7).

$$w_p = \int d\varepsilon_v + \int \eta d\varepsilon_s \quad (7)$$

Here η is the stress ratio that q is divided by p' . The volumetric strain is assumed to be zero in any undrained shearing. The equation (7) can be replaced by following equation (8).

$$w_p = \int \eta d\varepsilon_1 \quad (8)$$

w_p can be determined from a cross sectional area at ε^* corresponding to $DA = 5\%$ in $\eta \sim \varepsilon_1$ curve. Figure 11 shows the calculating example of w_p . Figure 12 shows comparison between w_p and w_1 . The numbers of data, n and the coefficient of correlation, r are given in this figure. There is a good correlation between w_p and w_1 . Instead of w_p , w_1 or w_2 could be used as index to represent the energy required to liquefaction or reliquefaction. Figure 13 shows comparison between w_1 and w_2 of both samples. It was shown that w_1 of the undisturbed samples becomes bigger than that of the disturbed samples. Figure 14 shows relationship of Δe to w_1 and w_2 for both samples. w_1 and w_2 of the disturbed samples become bigger than those of the undisturbed samples. On the contrary, Δe of the disturbed samples is bigger than that of the undisturbed samples. Consequently the change in void ratio of the undisturbed sample is lesser than that of the disturbed samples during reconsolidation. However the first liquefaction needs lesser energy than the reliquefaction.

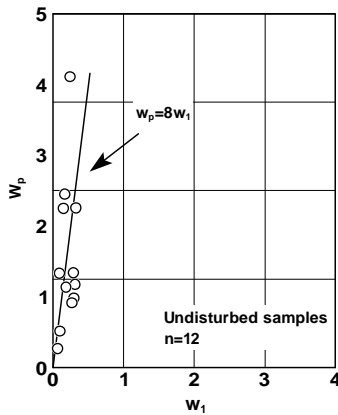


Figure 12 Comparison between w_p and w_1

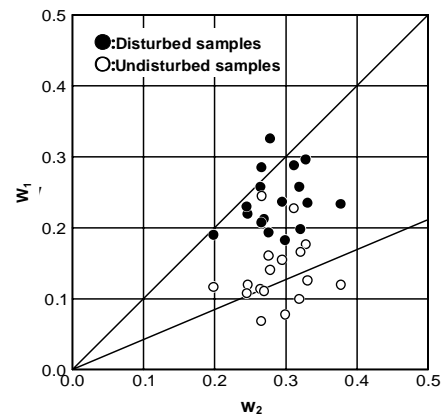


Figure 13 Relationship between w_1 and w_2

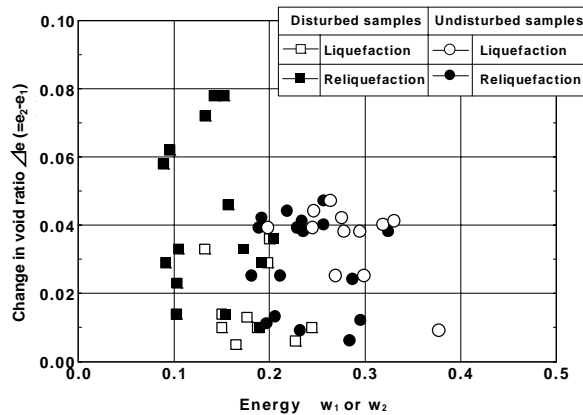


Figure 14 Relationship of Δe to w_1 and w_2

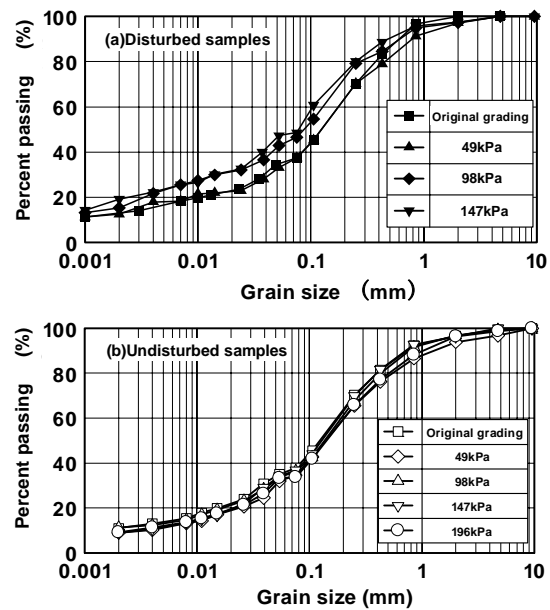
CHANGES OF GRADING AND MICROSTRUCTURE OF SOIL DUE TO CRUSHABILITY

Change in fine content after liquefaction

It is necessary to pay attention to change of physical property of sample due to particle crushing. Also it is important to grasp the meaning of qualitative and quantitative change of microstructure of the undisturbed sample. Grain size analysis were carried out on each sample when cyclic triaxial test had finished at $n_1=20$. Grading curves of the undisturbed and the disturbed samples are shown in Figures 15 (a) and (b). In the case of the disturbed samples, except for $\sigma_{30}'=49$ kPa, each grading curve moves toward the right side. This may be caused by particle crushing. The particle crushing produced an increase in the fine content of the sample. In the case of the undisturbed sample, the particle crushing seems not to remarkably occur as compared with the disturbed samples, irrespective of magnitude of σ_{30}' . Miura et al [13] reported that fine content, F_C is regarded as index to represent degree of particle crushing and F_C is relates to an increase in surface area of soil particle due to particle crushing. Figure 16 shows relationship between a change of F_C , ΔF_C and σ_{30}' . ΔF_C of the disturbed sample increases with an increase in σ_{30}' . At this time, the amount of ΔF_C becomes about 12 %. On the other hand, ΔF_C of the undisturbed samples has a similar tendency to the disturbed samples and becomes about 2.5 %. The total amount of ΔF_C of the undisturbed sample is lesser than that of the disturbed sample. The disturbed samples arose much particle crushing than the undisturbed samples.

Observation of microstructure using SEM

Photographs 2 (a) and (b) show the features of the disturbed specimen after consolidation and liquefaction using SEM, respectively. The observed sample was made from the specimen when cyclic triaxial test was carried out under $\sigma_{30}'=49$ kPa. As can be seen form Photos.2 (a), it was shown that the soil consists of angular volcanic glasses and coarse porous pumices. There exist a lot of fine particles among volcanic glasses. The diameter of the fine particle is the range of 1 μm to 10 μm . It could not been judged from only these photographs that the fine content after liquefaction increased as compared with after consolidation.



Figures 15 Change of grading curve due to liquefaction

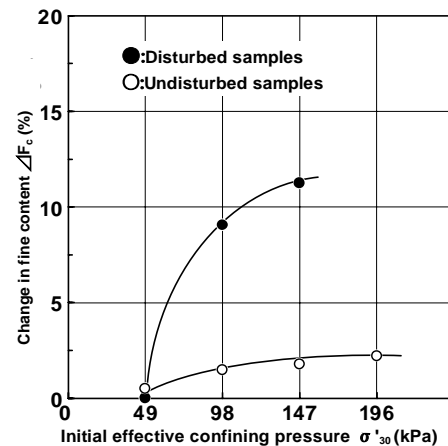
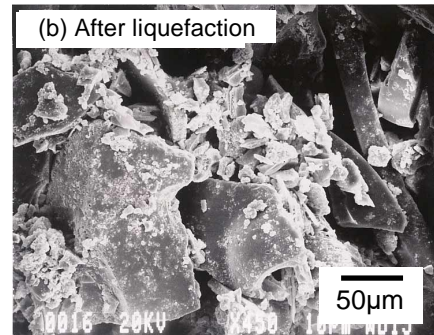
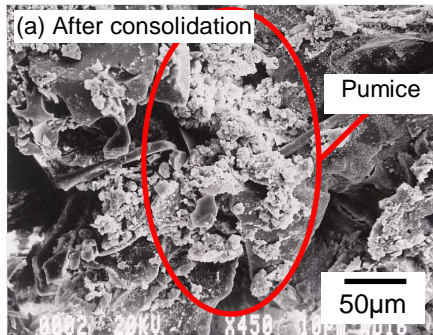


Figure 16 Relationship between change of fine content and initial effective pressure

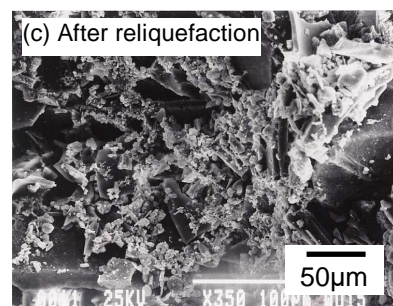
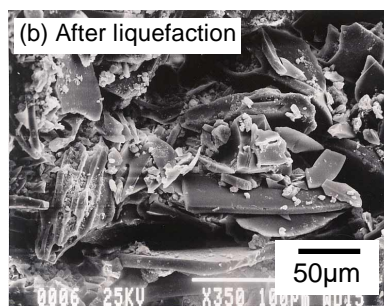
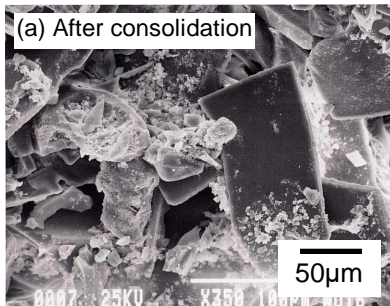
Photographs 3 (a) and (b) show the features of the undisturbed specimen after consolidation and liquefaction under $\sigma_{30}'=49$ kPa, respectively. There exists pumice (dia. 10 μm) around angular volcanic glasses. This fabric is resultant from cementation between particles. Such pumice is not observed after liquefaction. The cementation may be lost by liquefaction. Photographs 4 (a) to (c) show the features of the undisturbed specimen after consolidation, liquefaction and reliquefaction under $\sigma_{30}'=98$ kPa, respectively. A lot of volcanic glass is observed in all micrographs. The maximum diameter of the volcanic glass seems to vary from 10 μm to 100 μm . The amount of the fine particle around the volcanic glass increased in sequence of testing such as consolidation, liquefaction and reliquefaction. Photographs 5 (a) to (c) show the features of the undisturbed specimen after consolidation, liquefaction and reliquefaction under $\sigma_{30}'=147$ kPa, respectively. After consolidation, a lot of volcanic glass is observed,



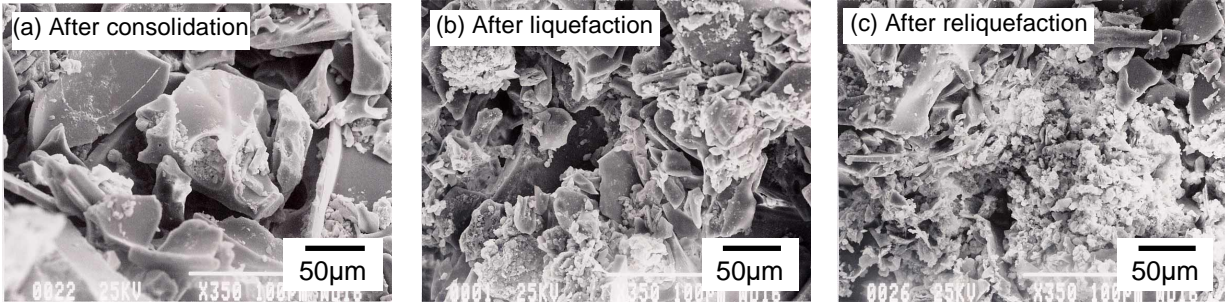
Photographs 2 SEM of disturbed samples ($\sigma_{30}'=98\text{kPa}$)



Photographs 3 SEM of undisturbed samples ($\sigma_{30}'=49\text{kPa}$)



Photographs 4 SEM of undisturbed samples ($\sigma_{30}'=98\text{kPa}$)



Photographs 5 SEM of undisturbed samples ($\sigma_{30}'=147\text{kPa}$)

but pumice is not observed. By comparing between Photos.5 (b) and (c), it was shown that the fine content of the sample remarkably increased after reliquefaction.

CONCLUSIONS

Main conclusions are summarized as follows.

- 1) The first liquefaction strength of the undisturbed sample becomes a higher value than that of the disturbed sample, independently of the initial effective confining stress.
- 2) The reliquefaction strength of the disturbed sample is equivalent to the first liquefaction strength, irrespective of the increase in void ratio due to reconsolidation.
- 3) The reliquefaction strength of the undisturbed sample becomes a lower value than the first liquefaction strength in the range of effective confining stress below 147 kPa, because of loss of bonding formed between soil particles.
- 4) The change in void ratio of the undisturbed sample after the first liquefaction is bigger than that of the disturbed sample.
- 5) There seems to be a unique relationship between the change in void ratio and the energy to cause liquefaction.
- 6) The change in fine content of both samples due to the crushability depends on the initial confining stress.

ACKNOWLEDGMENT

We wish to express our sincere thanks to Prof. Takumi OKABAYASHI (Kagoshima National College of Technology) for preparation of soil sample, to Mr. Osami YAMAMOTO (Yamaguchi University) for technical support, and to Mr. Takayuki SENDA, Mr. Takayuki SASANISHI and Ms. Ayumi YOSHIMORI for experimental assistance.

REFERENCES

1. Umehara, Y., Zen, K., Hamada, K. "Engineering properties of Shirasu for construction materials (Part-5) Dynamic properties based on dynamic triaxial tests." *Technical Note of the Port and Harbour Research Institute*, Ministry of Transport, Japan, (211), 79-101, 1975(*in Japanese*).
2. Yamanouchi, T. "Ground failure due to the Ebino earthquake." Report of the JSSMFE Technical Committee on Shirasu, *Tsuchi-to-Kiso*, JSSMFE, 16(9), 47-59, 1968(*in Japanese*).

3. Okabayashi, T., Hyodo, M., Murata, H., Yamamoto, T., Nakata, Y., Kitamura, R., Kobayashi, T., Fujii, T., Kusakabe, S. "Geotechnical property of the 1997 Kagoshimaken-hokuseibu and Daini-hokuseibu earthquakes." Western Regional Division Report of Japan Group for the Study of Natural Disaster, (22), 21-28, 1998(in Japanese).
4. Yamamoto, T., Okabayashi, T., Matsumoto, N. "Earthquake disaster in the 1997 Kagoshimaken-hokuseibu and Daini-hokuseibu earthquakes." *Japan Society for Earthquake Engineering Promotion News*, (157), 31-41, 1997(in Japanese).
5. Hyodo, M., Hyde, A.F.L., Aramaki, N. "Liquefaction of crushable soils." *Geotechnique*, 48(4), 527-543, 1998.
6. O-hara, S., Yasunaga, F., Fujii, N. "Dynamic behavior of undisturbed Shirasu." *Soils and Foundations*, 14(4), 107-114, 1974(in Japanese).
7. Okabayashi, T., Hyodo, M., Yasufuku, N., Murata, H. "Monotonic and cyclic undrained shear behavior of volcanic soil "Shirasu"." *Journal of Geotechnical Engineering, JSCE*, 499(28), 98-106, 1994(in Japanese).
8. Nakata, Y., Hyodo, M., Kato, Y., Murata, H. "Mechanical properties of crushable soils." *Tsuchi-to-Kiso, JSSMFE*, 48(10), 31-34, 2000(in Japanese).
9. Finn, W.D.L., Bransby, P.L., Pickering, D.J. "Effect of strain history on liquefaction of sand." *Journal of the Soil Mechanics and Foundation Division, ASCE*, 96(6), 1917-1934, 1970.
10. Yasuda, S., Tohno, I. "Sites of reliquefaction caused by the 1983 Nihonkai-Chubu earthquake." *Soils and Foundations*, 28(2), 61-72, 1988.
11. O-hara, S., Yamamoto, T. "Experimental studies on reliquefaction characteristics of saturated sands, using shaking table." *Soils and Foundations*, 22(2), 123-132, 1982(in Japanese).
12. JSSMFE, "Special soil in Japan", 213, 1974(in Japanese).
13. Miura, S., Yagi, K., Kawamura, S. "Static and cyclic shear behavior and particle crushing of volcanic coarse grained soils in Hokkaido." *Journal of Geotechnical Engineering, JSCE*, 547(36), 159-170, 1996(in Japanese).